Tilt-angle, polarization, and heat-capacity measurements near the smectic-A—chiral-smectic-C phase transition of p-(n-decyloxybenzylidene)-p-amino-(2-methylbutyl)cinnamate (DOBAMBC)

S. Dumrongrattana,* C. C. Huang, G. Nounesis, S. C. Lien,† and J. M. Viner‡
School of Physics and Astronomy, University of Minnesota, Minneapolis, Minnesota 55455
(Received 20 March 1986)

High-resolution heat-capacity, tilt-angle, and polarization measurements have been carried out in the vicinity of the smectic-A (SmA) —chiral-smectic-C (SmC^*) phase transition of p-(n-decyloxybenzylidene)-p-amino-(2-methylbutyl)cinnamate (DOBAMBC). Heat-capacity studies were done on two different samples obtained from two laboratories. Different results were obtained. Almost simultaneous measurements of the tilt angle (θ) and polarization (P) on one of the samples allow us to reveal one surprising temperature dependence of the ratio P/θ. The anomaly in the ratio P/θ seems to be closely related to the anomaly in the helical pitch just below the SmA-SmC^* transition.

I. INTRODUCTION

A variety of organic compounds exhibit the smectic-A (SmA) and, at lower temperature, the smectic-C (SmC) liquid-crystal phase characterized by a one-dimensional density wave which has a wave vector along (A), or tilted with respect to (C) the average long molecular axis (the director). If the constituent molecules are optically active, the chiral-smectic-C (SmC^*) phase will be observed instead of the SmC phase. Since 1975 Meyer *et al.*[1] established the existence of and investigated the behavior of a "pseudoproper" ferroelectric liquid crystal which showed the SmC^* phase in p-(n-decyloxybenzylidene)-p-amino-(2-methylbutyl) cinnamate (DOBAMBC), considerable experimental and theoretical effort has been put into characterizing the bulk properties of the SmC^*. In 1980, Clark and Lagerwall[2] demonstrated bistability and submicrosecond switching in thin SmC^* sample cells (thickness is about 1—2 μm). Thus the problem of carefully characterizing the bulk properties of the SmC^* is not just academic, it has important technological implications as well.

In late 1960 lack of proper methods to align the liquid-crystal molecules in the nematic phase impeded the progress of the careful experimental work and limited our understanding of this important liquid-crystal mesophase. A similar situation has happened to the SmC^* phase. Up to now, the majority of experimental work on the SmC^* phase has been carried out on multidomain samples with domain size $\lesssim 1$ mm^2. Consequently, large variances exist among the reported data. Recently, we have employed a surface alignment technique, developed by Patel and coworkers,[3] to prepare large-area single-domain DOBAMBC samples of area 12 mm$\times$18 mm and thickness 25 or 75 μm. Additional complications in characterizing the chiral-smectic-C materials originate from the fact that most of the published data are on the compounds like DOBAMBC which is a Schiff-base compound and is chemically unstable. Here we choose DOBAMBC mainly for the availability of the samples from a commercial supply and of various data for comparison. However, our carefully designed experimental procedures, i.e., almost simultaneous measurements on tilt angle (θ) and polarization (P), significantly reduce the effect due to the chemical instability in uncovering the important anomaly of the ratio (P/θ) just below the SmA-SmC^* transition temperature. In the near future, we plan to study some stable chiral-smectic-C compounds.

The samples with good alignment enable us to perform high-resolution measurements on the spontaneous polarization ($\pm 0.5\%$) and tilt angle (1.7×10^{-3} rad) with 3-mK temperature resolution.[4] In addition, electrical critical field studies were done on a commercial hot stage with 0.1-K temperature resolution[5] All these experiments were carried out on the samples purchased from Frinton Laboratories.[6] Meanwhile, high-resolution ac calorimetry measurements were performed on two different DOBAMBC samples from two different laboratories.

In Sec. II we shall present the extended mean-field theory for the SmA-SmC (SmC^*) transition. This will provide the theoretical basis for the discussion of our heat-capacity results in Sec. III. In Sec. IV measurement techniques and results of our tilt-angle and spontaneous polarization studies will be given. We will conclude our work with highlights of our experimental results in Sec. V. A generalized mean-field model will be presented in the following paper[7] to explain the anomalous behavior in P/θ and helical pitch anomaly in the SmC^* phase. Also we have successfully obtained all the mean-field coefficients.

II. EXTENDED MEAN-FIELD MODEL FOR THE SmA-SmC (SmC^*) TRANSITION

Based on their high-resolution heat-capacity studies near the SmA-SmC transition of one liquid-crystal compound, Huang and Viner[8] have proposed the following extended mean-field model to describe the SmA-SmC transition:

$$G=G_0+at\theta^2+b\theta^4+c\theta^6 . \quad (1)$$

Here G_0 is the background free energy without the SmA-SmC transition, the reduced temperature $t=(T-T_c)/T_c$, T_c is the SmA-SmC transition temperature, and the coefficients (a, b, and c) are positive constants for a continuous transition. The variable θ is the molecular tilt angle from the smectic layer normal and the magnitude of the smectic-C order parameter, i.e., $\Psi=\theta e^{i\phi}$, where ϕ is the azimuthal angle for the molecular tilt. Now minimizing the free energy with respect to θ, we have $\theta=0$ for $T>T_c$ and

$$\theta=[R(1-3t/t_0)^{1/2}-1]^{1/2} \quad (2)$$

for $T<T_c$, where $R=b/3c$ and $t_0=b^2/ac$. Substituting Eq. (2) into Eq. (1), the heat capacity can be calculated from $C=-T(\partial^2 G/\partial T^2)$ and

$$C=\begin{cases} C_0 , & (3a) \\ C_0+AT(T_m-T)^{-1/2} . & (3b) \end{cases}$$

Here C_0 is the background heat capacity derived from the background free energy G_0 which should vary smoothly through the transition, $A=a^{3/2}/[2(3c)^{1/2}T_c^{3/2}]$ and $T_m=T_c(1+t_0/3)$, where T_c is chosen to be the midpoint of the mean-field heat-capacity jump. The size of the mean-field heat-capacity jump at T_c is $\Delta C_J=a^2/(2bT_c)$. In the reduced temperature scale, the dimensionless parameter t_0 ($=b^2/ac$) is equal to the full width at half height of the $\Delta C/T$ versus T curve. Here $\Delta C=C-C_0$ is the anomalous part of the heat-capacity curve. Because of a wide temperature range for our data, we used $C_0=B+Dt+Et^2$ as the background term. To a fairly good approximation (within about 1%), the free energy in Eq. (1) can be used to describe the temperature dependence of heat capacity and tilt angle in the vicinity of the SmA-SmC^* transition. Details of this discussion will be made as part of the presentation of a generalized mean-field free energy for the SmA-SmC^* transition in the following paper.[7]

From Eq. (2), an important property associated with the dimensionless parameter t_0 can be obtained. For $|t| \ll t_0$, $\theta \sim |t|^{1/2}$ and $|t| \gg t_0$, $\theta \sim |t|^{1/4}$, thus t_0 characterizes the crossover from an ordinary mean-field region $|t| \ll t_0$ to a tricritical-like region $|t| \gg t_0$. In all high-resolution studies near the SmA-SmC transition,[8,9] one finds that t_0 values (to date) approximately lie in the range $(1-6)\times 10^{-3}$. With transition temperatures being approximately equal to 350 K, the crossover from $\theta \sim |t|^{1/2}$ to $\theta \sim |t|^{1/4}$ occurs around $T_c-T \simeq 1$ K. This explains why the reported results on the critical exponent β associated with the tilt angle vary so much from one experiment to the other one. An evolution of the effective critical exponent β in a $\log(\theta)$ versus $\log(t)$ plot is one of the important features of the extended mean-field model.[10]

Furthermore, within the mean-field model, one can derive a unique relationship between the amplitude of the order parameter (θ) and the anomalous part of heat capacity ΔC ($=C-C_0$),[11] i.e.,

TABLE I. Summary of the heat-capacity data analyses near the SmA-SmC^* transition of sample I. Here the coefficient a is set equal to one (see Refs. 16 and 17). * means that the corresponding parameter has been set equal to zero in the given fitting. Fitting range for case A is $1.6 < T-T_c < 8.4$ K and $1.6 < T_c-T < 12.6$ K, and that for case B is $1.6 < T-T_c < 8.4$ K and $0.1 < T_c-T < 12.6$ K. For the convenience of our fitting the coefficient a is set equal to one and the units of the angle θ become $(\mathrm{J/m^3})^{1/2}$. This leads to the unusual units of $(\mathrm{J/m^3})^{-1}$ and $(\mathrm{J/m^3})^{-2}$ for the coefficients b and c, respectively. Only in this case, we have these unusual units for a, b, c, and θ. The rest of the paper, θ has units rad and the coefficients a, b, and c have units $\mathrm{J/m^3}$.

Case	$10^4 b$	$10^5 c$	$10^8 d$	χ^2
A	4.5±0.1	6.3±0.2	*	1.0
	4.5±0.1	6.3±0.2	0.2	1.0
B	3.1±0.2	6.8±0.4	*	3.0
	3.1±0.2	6.8±0.4	1.3	3.0

$$\theta=\left[\frac{T_c}{a}\int_T^{T_c}\frac{\Delta C}{T}dT\right]^{1/2} . \quad (4)$$

Such a simple relation does not exist in the three dimensional (3D) XY model in which $\theta \sim |t|^{0.35}$ and $\Delta C \sim |t|^{-0.02}$. Thus with our high-resolution results on both the heat capacity and tilt angle, Eq. (4) will provide a crucial test for the validity of the mean-field theory in describing the SmA-SmC^* transition of DOBAMBC.

Finally, the following three relations—$t_0=b^2/(ac)$, $\Delta C_J=a^2/(2bT_c)$, and $R=b/(3c)$—enable us to calculate all three free-energy expansion coefficients, i.e., a, b, and c from the tilt-angle and heat-capacity data. $a=2T_c t_0(\Delta C_J)/(3R)$, $b=at_0/(3R)$, and $c=b/(3R)$. Naturally, the magnitudes and units for these three coefficients depend on the unit we choose for the tilt angle θ. Namely, if we scale the tilt angle $\tilde{\theta}$ by a constant factor F, i.e., $\tilde{\theta}=\theta/F$, then the corresponding free energy should not be changed and the free-energy expression [Eq. (1)] with $\tilde{\theta}$ being a variable instead of θ will have coefficients $\tilde{a}=aF^2$, $\tilde{b}=bF^4$, and $\tilde{c}=cF^6$ (Ref. 12). Except in our discussion of Table I, throughout this and the following paper the θ will have units rad, and a, b, and c will have units $\mathrm{J/m^3}$.

III. HEAT-CAPACITY MEASUREMENTS

Details of our ac calorimetry technique have been published before.[13] Since the extended mean-field model[8] was proposed, many research groups have carried out high-resolution heat-capacity measurements to check the specific expression for the anomalous part of the heat capacity i.e., Eq. (3). Here we have performed calorimetry studies on two different DOBAMBC samples prepared in two different laboratories. One of them (sample I) was synthesized by P. Keller at Orsay and given to us by R. Pindak. The other one (sample II) was purchased from Frinton Laboratories and recrystallized twice from

methanol by us. Sample I has been used by various research groups for many different studies related to the SmA-SmC^* phase transition or properties of the SmC^* phase. On the other hand, because only a very limited quantity of sample I (about 80 mg) was available, all our other measurements, i.e., tilt angle, spontaneous polarization, and electrical critical field, were done on sample II.

For example I, both electrical resistance heating[13] and optical heating techniques[14] were employed as the ac heating source in our ac calorimetric investigations. The optical heating scheme provided us with high quality and reproducible results. For some unknown reasons, the electrical resistance heating technique on sample I would not give us reproducible results for repeated measurements; we only used this measurement to obtain the heat-capacity jump in the vicinity of the transition which turned out to be reproducible within 10%. Our measured heat-capacity jump is 0.26 ± 0.03 J/cm^{3}K. The transition temperature T_c is about 94.6°C with a small T_c shift rate ($\sim$2 mK/h). All the data have been adjusted for this T_c shift, assuming that the shift rate was constant during our entire experimental run which lasted about 8 h. Our data with a resolution better than 0.1% is shown in Fig. 1. Here $T_c=367.722$ K, which is the midpoint of the heat-capacity jump.

Attempts at fitting all the data, except those just above T_c showing some rounding,[15] to Eq. (3) consistently gave us a relatively large value in χ^2. Actually, by increasing the excluded region for data fitting from 0.1 to 1.6 K for $T<T_c$, χ^2 decreased from 3.0 to 1.0. This suggests some unusual behavior even for $T<T_c$. To fully understand it, the background term C_0 was determined by fitting the data for $T>T_c$ between 369.33 and 376.15 K to Eq. (3a). The anomalous part of the heat capacity ΔC was obtained by subtracting the above background term from the measured value of C. The heat-capacity jump ΔC_J was found to be 3.38 in relative units from the maximum and minimum in the $\Delta C/T$ versus T curve near T_c. Then in the reduced temperature scale the full width at half height of the $\Delta C/T$ versus T curve gave $t_0=2.5\times10^{-3}$. Figure 2 shows a log-log plot of $\Delta C/T$ versus (T_m-T), where T_m was calculated from $T_m=T_c(1+t_0/3)=368.028$ K. The coefficient A in Eq. (3b) was then determined using $A=[t_0/(3T_c)]^{1/2}\Delta C_J=5.09\times10^{-3}$. The straight line (Fig. 2) calculated from $\Delta C/T=A(T_m-T)^{-1/2}$ [Eq. 3(b)] compares nicely with the data for $T_m-T>1.8$ K. However, a clear systematic deviation occurs for $T_m-T\lesssim1.5$ K. Near the heat-capacity peak the measured heat capacity is about 18% above the fitted curve. Consequently, in sample I for $|T-T_c|>1.6$ K the data are consistent with the extended mean-field expression. An excess heat capacity C_{ex} above the mean-field heat-capacity anomaly, in particular, for $T<T_c$ is found in the vicinity of the transition temperature.

The presence of excess heat capacity means that ΔC_J was overestimated and t_0 underestimated in the above data analysis. To improve the determination of t_0, ΔC_J, and the excess heat capacity, the heat-capacity data for $T<T_c$ and $T>T_c$ were fit simultaneously to the total mean-field heat-capacity expression [Eqs. (3a) and (3b)] in the temperature range $|T_c-T|>1.6$ K (the region of negligible excess heat capacity) with A, T, D, and E as adjustable parameters. Figures 1(a) and 1(b) show the best fit as a solid line. From $T_m=368.115$ K and $A=5.16\times10^{-3}$, then $t_0=3(T_m/T_c-1)=3.2\times10^{-3}$ and $\Delta C_J=(3T_c/t_0)^{1/2}A=3.03$ were obtained. The value of t_0 is comparable to those of other SmA-SmC (or SmC^*) transitions.[16] By reducing the excluded region from 1.6 to 0.5 K or 0.1 K for $T<T_c$, χ^2 increases from 1.0 to 1.5 and 3.0, respectively. This is consistent with our observation that near T_c there exists excess heat capacity in the sample I. Next, we have also carried out fittings of our

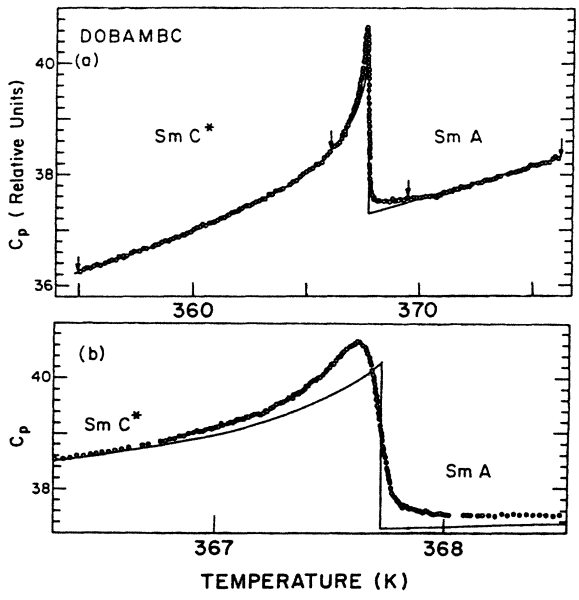

FIG. 1. (a) Total heat capacity (C_p) vs temperature (T) near the SmA-SmC^* transition of DOBAMBC (sample I). (b) C_P vs T on an expanded temperature scale. On the reduced temperature scale the width between 90% and 10% of the heat-capacity jump on the high-temperature side of the transition is 3×10^{-4}. Open circles are the data. The continuous lines are the best fit to Eqs. (3a) and (3b), simultaneously, in the regions between the arrows for $T<T_c$ and $T>T_c$, respectively.

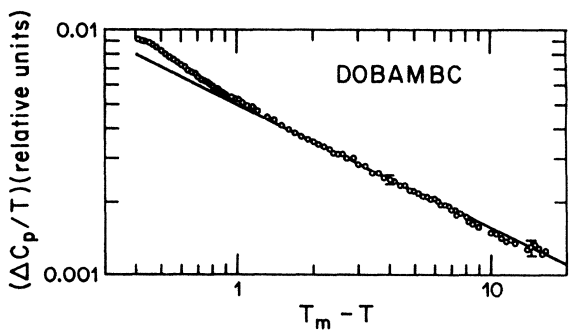

FIG. 2. Log-log plot of $(\Delta C_p/T)$ vs (T_m-T) for $T<T_c$ of sample I. See the text for the definition of T_m. The solid line is calculated from the known parameters for $A(T_m-T)^{-1/2}$. Typical uncertainties for two datum points are shown.

TABLE II. The relative magnitudes of the three expansion terms in the free energy with respect to $|at|\Psi|^2|$ term for the fitting results obtained in the case B of Table I. Here C is the ratio calculated at $T_c-T=0.1$ K, D is the ratio calculated at $T_c-T=12.6$ K.

	$\frac{b\|\Psi\|^4}{\|at\|\Psi\|^2\|}$	$\frac{c\|\Psi\|^6}{\|at\|\Psi\|^2\|}$	$\frac{d\|\Psi\|^8}{\|at\|\Psi\|^2\|}$
C	0.45	0.034	2.2×10^{-5}
D	0.11	0.27	5.8×10^{-3}

heat-capacity data to a heat-capacity expression derived from a free energy including one additional term, i.e., $d|\Psi|^8$, to that of Eq. (1). Because this mean-field expression still cannot account for the excess heat capacity above T_c, we exclude the region $0<T-T_c<1.6$ K from our fittings. The results are summarized in Table I. It is clear that the fitting results are fairly insensitive to the $|\Psi|^8$ term and including the data in the region $0.1<T_c-T<1.6$ K increases χ^2 from 1.0 to 3.0. To demonstrate relative importance of each term in the mean-field free-energy expansion, the ratios of three expansion terms in the free energy to $|at|\Psi|^2|$ term are listed in Table II for two cases. Consequently, the $|\Psi|^8$ term cannot explain the excess heat capacity we have observed here for $T<T_c$. Although one may argue that the observed excess heat capacity may be due to the smearing out of a weakly first-order phase transition, this possibility is ruled out based on the very small phase change ($<3\times10^{-2}$ rad) observed through the SmA-SmC^* transition. Because of the T_c drift in this Schiff-base compound, it is not easy to measure thermal hysteresis.

To provide essential information for the free energy in describing the SmA-SmC^* transition, we have carried out heat-capacity, tilt-angle, spontaneous polarization, and electrical critical field measurements on sample II. The temperature dependence of heat capacity with ac electrical heating technique is displayed in Fig. 3. Except for some rounding in the immediate neighborhood of the transition temperature, the heat-capacity expression [Eq. (3)] derived from the extended mean-field theory gave a very good fitting to the data. The fitted curve is shown in Fig. 3 as a solid line. The important parameters, i.e., heat-capacity jump (ΔC_J), t_0, transition temperature (T_c), and T_m are shown in Table III for comparison with the results from sample I. Here both ΔC_J and t_0 are quite different for sample I and sample II. Because of the lack of high-resolution tilt-angle data on sample I, it is impossible to make further comparison of the mean-field expansion coefficients between these two samples. At this moment, we cannot account for the variance in ΔC_J and t_0 from different samples except that LeGrange and Mochel[18]

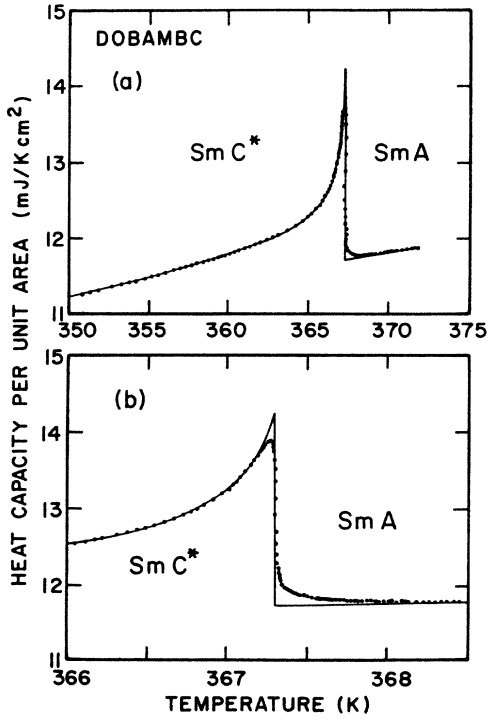

FIG. 3. Heat capacity per unit area (sample thickness 72 μm) as a function of temperature near the SmA-SmC^* transition of sample II. Solid circles, experimental data; solid line, best fit to Eq. (3). (a) The entire set of experimental data is plotted, (b) The data close to T_c are displayed to show the rounding effect near T_c. The heat-capacity jump is sharper than that of sample I. In the reduced temperature scale the width between 90% and 10% of the heat-capacity jump on the high-temperature side of the transition is 1.9×10^{-4}.

have obtained very different critical behaviors for the nematic-SmA transition of octyloxycyanobiphenyl (80CB) from two different batches of samples provided by the same supplier, British Drug Houses. Also, the fact that sample I has the excess heat capacity above the mean-field heat-capacity anomaly in the region $T<T_c$ but sample II does not, cannot be explained. Furthermore, our results show that sample I has higher values of T_c and T_m than sample II does. Except that sample II has a sharper heat-capacity jump on the high-temperature side of the transition than sample I does, we do not have any independent chemical analysis results to assess the impurity level of our samples. On the reduced temperature scale the width between 90% and 10% of the heat-capacity jump on the high-temperature side of the transition is 3×10^{-4} for sample I and 2×10^{-4} for sample II.

TABLE III. The measured parameters t_0 and ΔC_J for samples I and II.

	$10^3 t_0$	$10^{-6}\Delta C_J$ (J/m^{3}K)	$10^{-3}t_0\Delta C_J$(J/m^{3}K)	T_c (K)	T_m (K)
Sample I	3.21	0.26±0.03	0.83±0.10	367.722	368.115
Sample II	1.42	0.35±0.03	0.50±0.05	367.300	367.474

IV. TILT-ANGLE AND SPONTANEOUS POLARIZATION MEASUREMENTS

A. Sample preparation

So far many experiments have been carried out to study the temperature dependence of tilt angle[19,20] and spontaneous polarization[19,21,22] in the SmC^* phase of DOBAMBC. The existing data are fairly scattered with large uncertainty. One of the major experimental difficulties is that large single-domain samples in the SmC^* phase could not be achieved before. Employing a new surface alignment technique developed by Patel *et al.*,[3] we can easily obtain single-domain samples of DOBAMBC with area 12 mm$\times$18 mm and thickness 25 or 75 μm. The essential steps in preparing the sample cells are the following. First the clean glass slide with indium-tin-oxide (ITO) coating was spin coated with a thin film of promoter and then thin nylon polymer film. After leaving the slide in ambient conditions for one day, unidirectional rubbing on cotton cloth will provide surface alignment force for the liquid-crystal molecules. The sample cell consists of one polymer-coated slide and another uncoated one with Mylar spacers of proper thickness in between. A 5-min epoxy was used to bound the sample cell together. After capillary sucking the DOBAMBC sample inside a vacuum chamber in its isotropic phase, the sample was allowed to cool through the isotropic-SmA transition with a rate 4 K/h and then down to the SmC^* phase with a rate about 20 K/h. Under a polarizing microscope, uniform and equal spacing dechiralization lines could be seen throughout the sample. This indicates the high quality of sample alignment. Next the electrical resistance of the sample was measured. If there were too many free ions, the resistance was low and the polarization would have low values with a larger uncertainty in data. The typical resistance for our good sample with thickness 25 μm is about 40 MΩ which is higher than the reported value.[23]

With one rubbed polymer surface, the liquid crystal will align more easily inside our sample cell. This allows us to fast cool the sample into the SmA and SmC^* phase and maintain excellent alignment. Because the sample stays a reasonably short time ($\lesssim$2 h) in the high-temperature regions (i.e., $T-T_c \gtrsim 10$ K), this helps us to reduce the deterioration of the sample. In the case of our heat-capacity measurement, the sample was heated up to the isotropic phase for only about 10 min and the sample was in the high-temperature regions $T-T_c \gtrsim 10$ K for less than 30 min. The SmA-SmC^* transition temperature (T_c) for sample II is 367.30 K from our heat-capacity measurements and 366.83 K from our tilt-angle and polarization studies. However, once we express the integration of the anomalous part of the heat capacity and tilt angle in terms of T_c-T with measured T_c's from those two experiments, those two quantities are proportional to each other as predicted by the extended mean-field model (see Sec. IV C for detailed discussion). This indicates that even though our measured T_c in the tilt-angle and polarization studies is lower, its effect on the measured physical properties is insignificant.

B. Experimental setup and measurement techniques

The block diagram of our experimental setup for the polarization and tilt-angle measurements is shown in Fig. 4. A Wavetek 182A function generator provides a triggering signal to a signal averager PAR4202 and a triangular wave to be amplified by a Kepco power supply and amplifier model BOP 1000M which provides a voltage to the sample "s" up to $\pm$1000 V. The total current through the sample is sensed by the voltage across a series resistor R_s (50 kΩ). This signal is then fed to the input of signal averager channel 1 to enhance the signal to noise ratio through repeated measurements. Then the displacement-current data from the signal averager are output to a minicomputer for data reductions through a buffer, which acts as a dc level shifter and amplifier. A laser source, cross polarizers, and an optical detector are used to detect the optical signal during field reversal to ensure that the sample is always well aligned during the experimental run. This optical signal is also averaged by the signal averager simultaneously with the displacement current. Both signals are then recorded by a chart recorder.

For tilt-angle measurements, the Kepco BOP 1000M also provides a dc voltage to the sample to unwind the helix. The rotating stage, on which the oven is attached, enables us to rotate the sample and look for the minimum optical signal when the average molecular direction is parallel to the cross polarizers. The accuracy of the rotating stage angular reading is 1 min. If the first reading is at an angle θ_1, reversing field will provide another reading θ_2. The tilt angle is obtained by dividing the difference of those two angles by two. Since the optical detector is a photodiode connected in series with an external resistor and a dc power source, the process of minimum signal detection is simply measuring the resistance of the photodiode. The very fast change of resistance of the photodiode in response to light intensity allows us to measure the tilt angle with resolution $\pm$5 min.

The temperature controller is operated in a resistance mode. The difference reading between the standard resistance setting and thermistor resistance inside the oven will send an error signal to control the power supply output to the heater and bring the temperature toward the reference setting value. Within 15 min after changing the standard resistance setting, this temperature control unit can stabilize the temperature of our oven better than $\pm$3 mK.

The spontaneous polarization is determined from measurements of the displacement current through a field-reversal method. The sample cell was driven by a triangular wave[23] instead of a square wave.[24] The linear background (triangular-wave method) instead of the exponential one (square-wave method) simplifies the data reduction a great deal.[23] Figure 5(b) shows one typical polarization displacement and background current at $T_c-T=1.2$ K with a triangular driving electrical field [Fig. 5(a)]. Three major contributions to Fig. 5(b) are the following. The capacitance of the sample leads to step at the point where the slope of the applied electric field changes sign. The constant slope part is due to the finite electrical resistance of the sample. Finally, the sharp peak and dip come

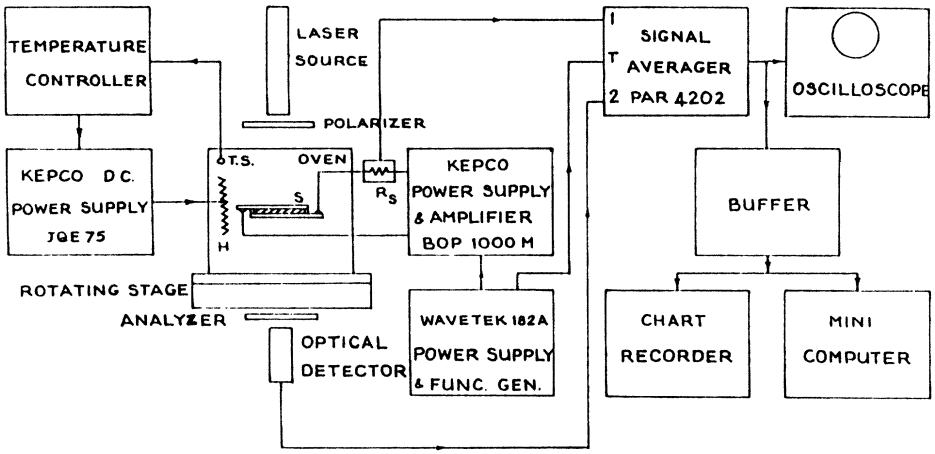

FIG. 4. Block diagram of the experimental set up for the polarization and tilt-angle measurements.

from the polarization displacement current when the applied electrical field changes sign. Figure 5(c) is the optical response curve measured by a photodetector. The sample was aligned such that the smectic layer normal was parallel to the optical axis of one of the cross polarizers. From our experience, a clean, nice optical response curve like Fig. 5(c) indicates that the quality of the sample alignment is maintained in the region where the laser beam passed through. Just below the SmA-SmC^* transition, the displacement current resulting from the bulk spontaneous polarization is very small. A signal averager was employed to enhance the signal-to-noise ratio. At our operating frequency (10 Hz), the spontaneous polarization was measured as a function of applied electric field strength (E) for $T_c - T = 1.0$ and 20.2 K. Figure 6 shows our result for $T_c - T = 20.16$ K. The measured polarization remains fairly constant (within 1%) for $E > E_p$. Here E_p is approximately equal to twice the critical field (E_u) to unwind the helix. Under the applied electrical field, the value of E_u was determined by observing the disappearance of helix under a polarizing microscope. Our entire polarization measurements were carried out at $E \simeq 2E_p$ (for $T_c - T = 20$ K) $= 2.5 \times 10^6$ V/m. A smaller polarization was obtained for $E < E_p$, because the helix is not fully unwound and/or the surface layers are not aligned. For $E > E_p$, the constancy of the measured polarization indicates that the electric field induced dipole moment will contribute to the background current instead of the displacement current peak which appears right after the value of E crossing the zero-field line.

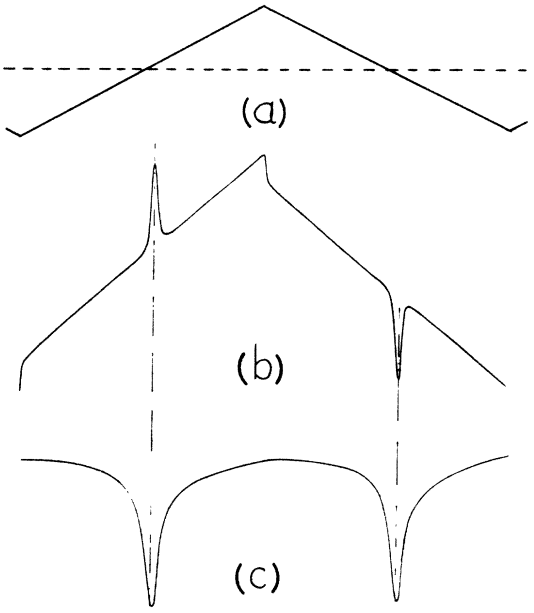

FIG. 5. (a) Triangular electric field ($E = 50$ V zero to peak) to drive the sample for the polarization measurements. (b) The polarization displacement and background current measured at $T_c - T = 1.2$ K. (c) Optical response relative to the polarization peak position.

C. Experimental results

A plot of our spontaneous polarization data versus temperature ($T_c - T$) is shown in Fig. 7. The data from the

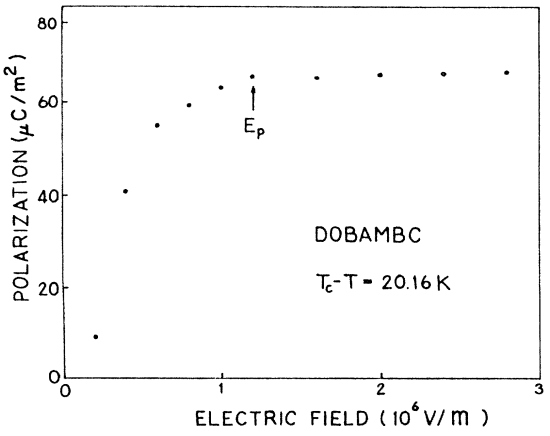

FIG. 6. The polarizations measured in various electric field at frequency 10 Hz and temperature 20.16 K below T_c. The sample thickness is 25 μm.

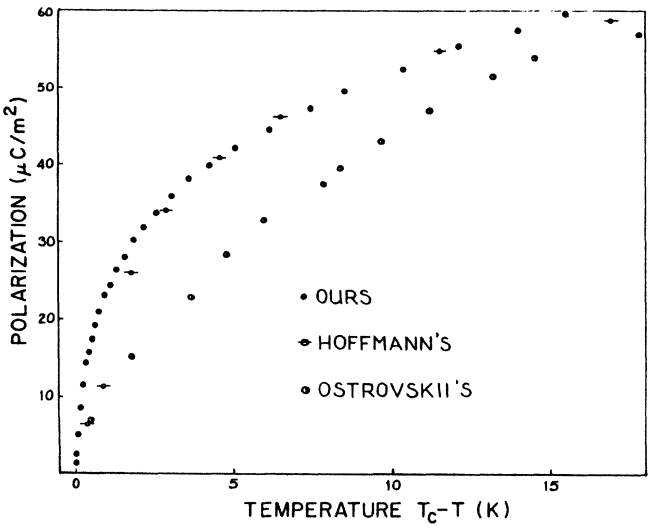

FIG. 7. Comparison of our polarization data with the previous results of Hoffman *et al.* (Ref. 21) and Ostrovskii *et al.* (Ref. 19). The values from Ref. 21 have been reduced to one-half.

work of Ostrovskii *et al.*[19] and Hoffmann *et al.*[21] are also shown in the same figure for comparison. As far as temperature-dependent behavior is concerned, our result is in reasonable agreement with the one reported by Hoffmann *et al.*[21] But our polarization values are lower by about one-half. The difference of our result from Ostrovskii's is not known exactly. However, from our measurements on various samples the major source of data deviation comes from the condition of the samples themselves. First, the domain walls increase the energy barrier of polarization rotation and reduce the measured polarization values. In this case the characteristic shape of the polarization versus temperature curve does not change very much provided the sample consists of a few large domains. Second, the electrical conductivity of the sample due to impurities causes a screening effect which can reduce the measured polarization tremendously, in the worst case, the polarization peak could disappear. This effect alone can severely change the shape of the polarization versus temperature curve. Our sample of area 2.2 cm^2 and 25 μm thickness has a high resistance about 40 MΩ. Our polarization values are usually higher than the previously reported values.[19,22] Surprisingly, the unaligned sample of Hoffmann *et al.* gave polarization values higher than ours by a factor of 2.

The electroclinic effect suggests that in the measurements of the tilt angle by field unwinding helical structure an extra induced tilt angle (θ_i) will be added to the zero-field tilt angle (θ_0). In order to reduce the finite field effect on the tilt angle, at a given temperature, the tilt angles were measured with at least four different applied electric fields. The tilt angle is obtained from an extrapolation to the zero-field limit. The transition temperature (T_c) in this measurement is determined from the temperature when a small hump of the spontaneous polarization peak starts to appear ($=93.68$ °C). In the vicinity of transition temperature the resolution of the tilt-angle measurement is very high (5×10^{-4} rad) when the tilt angle is small and the resolution decreases to about 1.7×10^{-3} rad when the temperature of the sample decreases far below T_c while the tilt angle is large. Therefore, our extrapolation could be done accurately.

Our tilt-angle data in comparison with the work of Ostrovskii *et al.*[19] and Martinot-Lagarde *et al.*[20] are shown in Fig. 8. Although all of these three sets of data are obtained from optical tilt measurements in the planar configuration, our result with a much higher resolution is in reasonable agreement with the one reported by Ostrovskii *et al.* who have used a high magnetic field of 17 kG to align the liquid-crystal molecules. Martinot-Lagarde *et al.*[20] employed the method of glass surface rubbing without a polymer coated layer. It is possible that the large deviation of the one reported by Martinot-Lagarde *et al.* from ours is due to the quality of sample alignment.

We have tried to perform a simple power-law fitting of our tilt angle and polarization, namely, $\theta=A_1(T_c-T)^\beta$ and $P=A_2(T_c-T)^\beta$. The data could not be fitted to the above expressions with any value of β in any reasonable temperature range. Moreover, the slope of the temperature dependence of the tilt angle and polarization in a log-log plot seems to vary from ~0.5 in the vicinity of T_c, to ~0.27 for far away from T_c (see Fig. 9). This result clearly indicates that the extended mean-field model by Huang and Viner[7] should be used.

With both heat capacity and tilt angle available from sample II, we should be able to test the important relation [Eq. (4)] derived from the mean-field model. First we integrate the anomalous part of the heat capacity to obtain

$$\theta_c \equiv \left[\int_T^{T_c} \frac{\Delta C}{T} dT\right]^{1/2} . \tag{5}$$

With ΔC in the unit of J/m^3 K [i.e., the heat capacity per

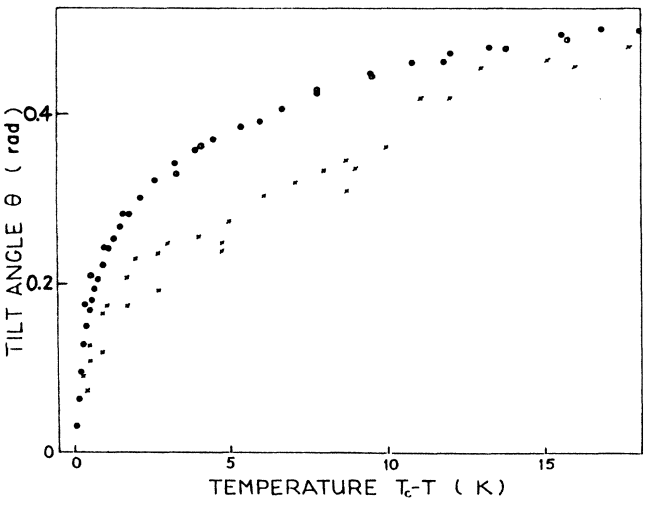

FIG. 8. Comparison of our tilt-angle data (denoted by solid circles) with the previous results by Ostrovskii *et al.* (half-open circles) (Ref. 19) and Martinot-Lagarde *et al.* (plus signs) (Ref. 20).

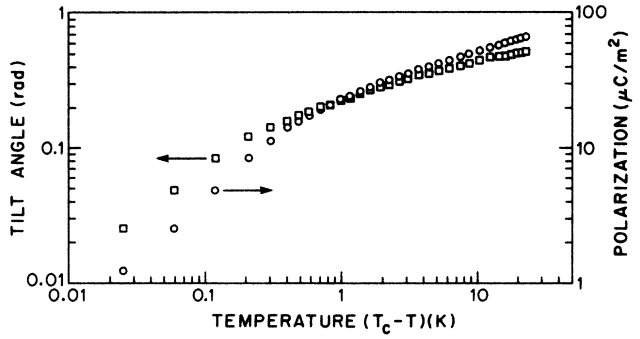

FIG. 9. Log-log plot of the polarization and tilt angle vs (T_c-T).

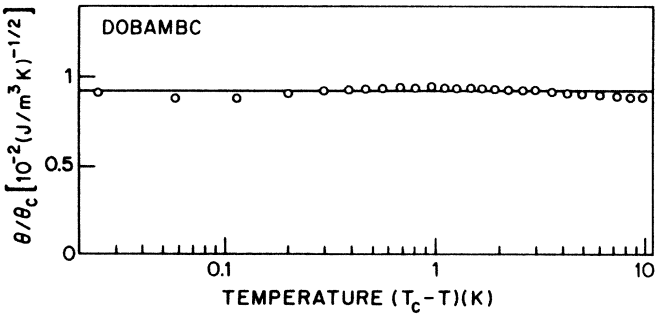

FIG. 11. The ratio θ/θ_c is plotted as a function of (T_c-T).

unit area displayed in Fig. 3 divided by the sample thickness ($=72\ \mu$m) (Ref. 25)], θ_c has the unit of $(J/m^3K)^{1/2}$. The result is shown in Fig. 10 with the measured tilt-angle data. The temperature dependence of θ_c looks similar to that of the tilt-angle data. In Fig. 11 the ratio θ/θ_c is plotted as a function of (T_c-T). It is obvious that θ/θ_c remains fairly constant over more than two and one-half decades in (T_c-T). This confirms the relationship in Eq. (4) and provides an additional strong support for the validity of the mean-field model in describing the SmA-SmC (or SmC^*) transitions. Comparing Eqs. (4) and (5), we have $\theta/\theta_c=(T_c/a)^{1/2}$. From this we obtain the leading coefficient in the Landau free-energy expansion, $a/T_c=1.13\times10^4$ J/m^{3}K. Another important observation one can make from Eq. (4) is that the anomalous part of the heat capacity is proportional to the temperature derivative of the tilt angle. Consequently, the heat capacity will have more-detailed features of the transition than the tilt angle. The existing data support this observation. Furthermore, it is much easier to measure the heat capacity with high resolution than to measure tilt angle. Thus to search for a fluctuation-dominated SmA-SmC (or SmC^*) transition, heat capacity would be a suitable quantity to study.

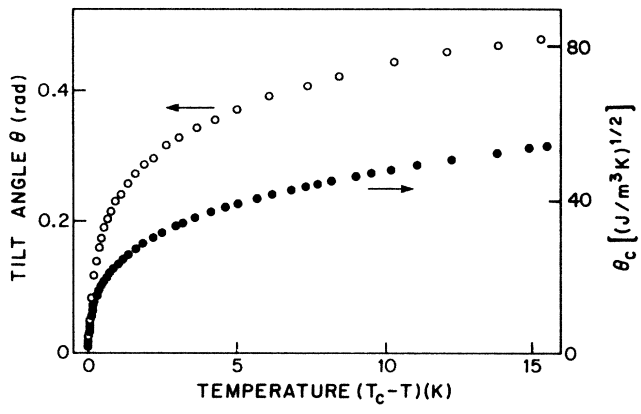

FIG. 10. Measured tilt angle (θ) (open circle) and calculated θ_c (solid circle) from our heat-capacity data are plotted as a function of (T_c-T). Here T_c's are measured values from respective studies which give small difference in T_c's. We believe that this is due to the amount of time the samples had to stay in the high-temperature region ($T-T_c\gtrsim10$ K) for given experimental requirement.

Now we can employ the value of constant a/T_c obtained from the ratio θ/θ_c and ΔC_J and t_0 determined from the heat-capacity fitting to obtain $3R=2(T_c/a)t_0(\Delta C_J)=0.089$. Then the coefficients b [$=at_0/(3R)$] and c [$=b/(3R)$] in the extended mean-field model become 6.60×10^4 J/m^3 and 7.4×10^5 J/m^3, respectively. For clear reference, the values of a, a/T_c, b, and c are listed in Table IV. Their relations with the similar sets of coefficients in the following paper are as follows: $a/T_c=\frac{1}{2}a_2=\frac{1}{2}a'$, $b=\frac{1}{4}a_4\simeq\frac{1}{4}b'$, and $c=\frac{1}{6}a_6\simeq\frac{1}{6}c'$. The differences between a_4 and b' as well as a_6 and c' are less than 1%. See the following paper for detailed discussion.

One of the problems in performing experiments on DOBAMBC is the T_c shift. In our polarization and tilt-angle measurements, the transition temperature shifted down with rate 20 mK/h. We assume that this rate was constant throughout our measurements. All the data reported here have been corrected for this T_c shift. In order to measure the ratio of the polarization (P) to the tilt angle (θ) with high resolution and confidence, we have performed these measurements one after the other for a given sample temperature. These almost simultaneous measurements on both polarization and tilt angle result in a surprising behavior in the temperature dependence of the ratio P/θ (see Fig. 12). The salient features are that the ratio P/θ decreases slowly with temperature for $T_c-T\gtrsim2$ K and shows a dramatic drop with temperature for $T_c-T\lesssim1$ K and reaches a finite value at $T=T_c$. This result contradicts the widely held belief that the ratio P/θ remains constant[26] or varies smoothly throughout the SmC^* phase.[19] This anomalous behavior in P/θ reminds us of the prevailing and well-known anomaly in the temperature variation of the SmC^* helicoidal pitch.[20,27]

TABLE IV. Three leading mean-field coefficients for sample II.

a/T_c (J/m^3 K)	a (J/m^3)	b (J/m^3)	c (J/m^3)
1.13×10^4	4.15×10^6	6.6×10^4	7.4×10^5

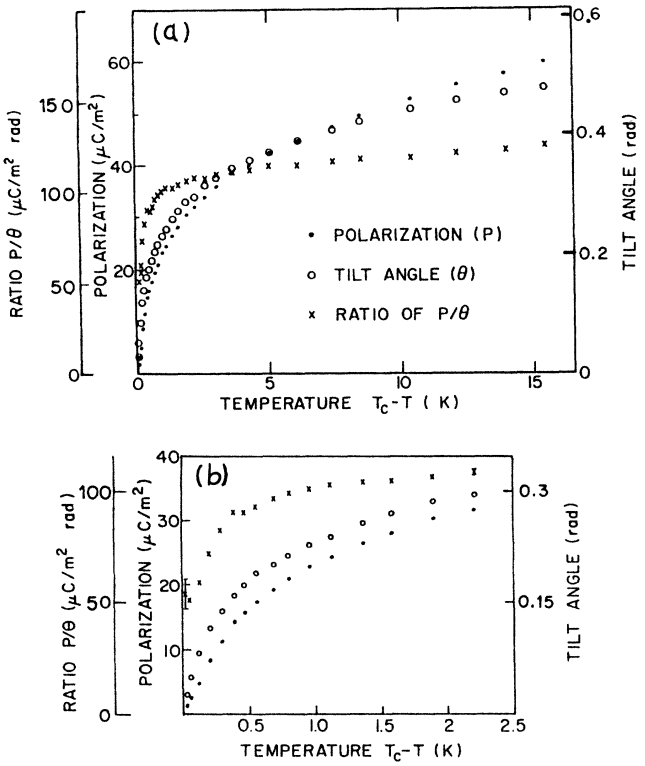

FIG. 12. Measured tilt angle θ, polarization P, and the ratio P/θ are plotted with temperature ($T_c - T$) in entire temperature range (a) and in the vicinity of T_c (b).

Experimentally, the pitches were found to increase very fast just below the SmA-SmC^* transition, reach a maximum around $T_c - T \lesssim 1$ K and then decrease slowly with decreasing temperature. In the light of our result on P/θ, we proposed a generalized mean-field model[4,7] to provide qualitative explanations for the temperature dependence of pitch and P/θ.

Because the anomalous behavior in q is fairly common among the chiral-smectic-C material,[20] we expect that the dramatic drop in the ratio P/θ just below the SmA-SmC^* transition is also a very common one. Finally, in performing the tilt-angle measurement, we have kept our applied voltage small enough such that $(1/8\pi)\epsilon E^2$ term is always smaller than the PE term. For example, at $T_c - T = 5$ K, $P = 42\ \mu\text{C/m}^2$, and $\epsilon = 2.1 \times 10^{-11}$ F/m (Ref. 28), with applied electric field $E = 2.5 \times 10^6$ V/m, we have $(1/8\pi)\epsilon E^2/(PE) \simeq 0.05$.

V. CONCLUSION

Our high-resolution heat-capacity and tilt-angle data satisfy the unique relation [Eq. (4)]. This combined with the measured heat-capacity anomaly provides a strong support for employing the mean-field theory in describing the SmA-SmC (or SmC^*) transition. The almost simultaneous measurements on the polarization and tilt angle reveal a surprising and unique temperature dependence of the ratio P/θ. This result leads us to propose a more complete mean-field theory for describing the SmA-SmC^* transition. Further measurements on the other SmC^* liquid-crystal compounds are in progress.

ACKNOWLEDGMENTS

We would like to thank T. Pitchford for much experimental help, J. Novack for helping us with the recrystallization process, and W. Huffman for providing the ITO-coated slides. This work was partially supported by a research contract from Minnesota Mining and Manufacturing Company (St. Paul, MN), the Center for Microelectronic and Information Sciences, University of Minnesota, and the National Science Foundation Solid State Chemistry Program, under Grant No. DMR-85-03419.

*Present address: King Mongjut's Institute of Technology, Thonburi, Pracha-Utit Road, Bangmod, Raj-Burana, Bangkok, Thailand.

†Present address: Energy Conversion Devices, Inc., Troy MI 48084.

‡Present address: Department of Physics, University of Utah, Salt Lake City, UT 84112.

[1]R. B. Meyer, L. Liebert, L. Strzelecki, and P. Keller, J. Phys. (Paris) Lett. **36**, 69 (1975).

[2]N. A. Clark and S. T. Lagerwall, Appl. Phys. Lett. **36**, 899 (1980).

[3]J. S. Patel, T. M. Leslie, and J. W. Goodby, Ferroelectrics **59**, 137 (1984).

[4]S. Dumrongrattana and C. C. Huang, Phys. Rev. Lett. **56**, 464 (1986).

[5]S. Dumrongrattana and C. C. Huang (unpublished).

[6]Frinton Laboratories, Inc. P. O. Box 2310, Vineland, NJ 08360.

[7]C. C. Huang and S. Dumrongrattana, following paper, Phys. Rev. A 34, 5020 (1986).

[8]C. C. Huang and J. M. Viner, Phys. Rev. A **25**, 3385 (1982).

[9]C. C. Huang and S. C. Lien, Phys. Rev. Lett. **47**, 1917 (1981); R. J. Birgeneau, C. W. Garland, A. R. Kortan, J. D. Litster, M. Meichle, B. M. Ocko, C. Rosenblatt, L. J. Yu, and J. Goodby, Phys. Rev. A **27**, 1251 (1983); M. Meichle and C. W. Garland, *ibid.* **27**, 2624 (1983); S. C. Lien, C. C. Huang, T. Carlsson, I. Dahl, and S. T. Lagerwall, Mol. Cryst. Liq. Cryst. **108**, 148 (1984); J. Theon and G. Seynhaeve, *ibid.* **127**, 229 (1985).

[10]C. C. Huang and J. M. Viner, in *Liquid Crystals and Ordered Fluids*, edited by A. C. Griffin and J. F. Johnson (Plenum, New York, 1984), Vol. 4, p. 643.

[11]S. Dumrongrattana, G. Nounesis, and C. C. Huang, Phys. Rev. A **33**, 2181 (1986).

[12]A proper choice of F for general discussions among the SmA-SmC (or -SmC^*) transitions in various liquid-crystal compounds was given in Ref. 16. Here, for the convenience of our discussions and comparison with the existing data, we will use the radian as the unit for θ in these two papers.

[13]J. M. Viner, D. Lamey, C. C. Huang, R. Pindak, and J. Goodby, Phys. Rev. A **28**, 2433 (1983).

[14]J. M. Viner and C. C. Huang, Solid State Commun. **39**, 789 (1981).

[15]The possible source of this rounding has been discussed in detail in Ref. 11.

[16]C. C. Huang and S. C. Lien, Phys. Rev. A **31**, 2621 (1985), and references found therein.

[17]Here, setting the leading coefficient $a=1$ means that we have properly chosen the order-parameter scale factor F such that $a\theta^2=\tilde{\theta}^2$ or $F=(1/a)^{1/2}$.

[18]J. D. LeGrange and J. M. Mochel, Phys. Rev. Lett. **45**, 35 (1980).

[19]B. I. Ostrovskii, A. Z. Rabinovich, A. S. Sonin, B. A. Strukov, and N. I. Chernova, Pis'ma Zh. Eksp. Teor. Fiz. **25**, 80 (1977) [JETP Lett. **25**, 70 (1977)].

[20]Ph. Martinot-Lagarde, R. Duke, and G. Durand, Mol. Cryst. Liq. Cryst. **75**, 249 (1981).

[21]J. Hoffmann, W. Kuczynsky, and J. Malecki, Mol. Cryst. Liq. Cryst. **44**, 287 (1978).

[22]H. Takezoe, K. Kondo, K. Miyasato, S. Abe, T. Tsuchiya, A. Fukuda, and E. Kuze, Ferroelectrics **58**, 55 (1984).

[23]K. Miyasoto, S. Abe, H. Takezoe, A. Fukuda, and E. Kuze, Jpn. J. Appl. Phys. **22**, L661 (1983).

[24]Ph. Martinot-Lagarde, J. Phys. (Paris) Lett. **38**, L17 (1977).

[25]The thickness of our sample reported in Ref. 11 should be 72 μm instead of 36 μm.

[26]R. B. Meyer, Mol. Cryst. Liq. Cryst. **40**, 33 (1977).

[27]B. I. Ostrovskii, A. Z. Rabinovich, A. S. Sonin, and B. A. Strukov, Zh. Eksp. Teor. Fiz. **74**, 1748 (1978); K. Kondo, H. Takezoe, A. Fukuda, and E. Kuze, Jpn. J. Appl. Phys. **21**, 224 (1982); R. Blinc, B. Zeks, I. Musevic, and A. Levstik, Mol. Cryst. Liq. Cryst. **114**, 189 (1984); I. Abdulhalim, L. Benguigui, and R. Weil, J. Phys. (Paris) **46**, 1429 (1985).

[28]D. S. Parmar and Ph. Martinot-Lagarde, Ann. Phys. (Paris) **3**, 275 (1978).